Neutron-scattering study of stripe-phase order of holes and spins in $La_{1.48}Nd_{0.4}Sr_{0.12}CuO_4$

J. M. Tranquada and J. D. Axe
Department of Physics, Brookhaven National Laboratory, Upton, New York 11973

N. Ichikawa, Y. Nakamura, and S. Uchida
Superconductivity Research Course, The University of Tokyo, Yayoi 2-11-16, Bunkyo-ku, Tokyo 113, Japan

B. Nachumi
Department of Physics, Columbia University, 538 West 120th Street, New York, New York 10027
(Received 29 February 1996)

We present a neutron diffraction study of charge and spin order within the CuO_2 planes of $La_{1.48}Nd_{0.4}Sr_{0.12}CuO_4$, a crystal in which superconductivity is anomalously suppressed. At low temperatures we observe elastic magnetic superlattice peaks of the type $(1/2\pm\epsilon,1/2,0)$ and charge-order peaks at $(2\pm2\epsilon,0,0)$, where $\epsilon=0.118$. After cooling the crystal through the low-temperature-orthorhombic (LTO) to low-temperature-tetragonal (LTT) phase transition near 70 K, the charge-order peaks appear first at ~60 K, with the magnetic peaks appearing below 50 K. The magnetic peaks increase in intensity by an order of magnitude below 3 K due to ordering of the Nd ions. We show that the observed diffraction features are consistent with stripe-phase order, in which the dopant-induced holes collect in domain walls that separate antiferromagnetic antiphase domains. The **Q** dependence of the magnetic scattering indicates that the low-temperature correlation length within the planes is substantial (~170 Å), but only very weak correlations exist between next-nearest-neighbor planes. Correlations between nearest-neighbor layers are frustrated by pinning of the charge stripes to the lattice distortions of the LTT phase. The spin-density-wave amplitude corresponds to a Cu moment of $0.10\pm0.03\ \mu_B$. The behavior of the electrical resistivity within the LTT phase is examined, and the significance of stripe-phase correlations for understanding the unusual transport properties of layered cuprates is discussed. [S0163-1829(96)01134-4]

I. INTRODUCTION

In trying to understand the copper-oxide superconductors, one of the key questions concerns the interaction between the magnetic moments associated with Cu^{2+} ions and the dopant-induced holes of O-2p-like character. Do the holes and the Cu spins combine to form a spatially homogeneous system, or is there a tendency for the charges to segregate, leaving behind locally antiferromagnetic domains? The first theoretical suggestions that the latter might be the case came from Hartree-Fock[1–6] and Monte Carlo[7,8] analyses of the single-band Hubbard model. These calculations yielded striped-phase solutions in which the holes collect in domain walls separating antiferromagnetic antiphase domains. Alternatively, evidence for charge segregation has been found in studies of the t-J model and of a lattice-gas model containing competing interactions.[9–11] More recent theoretical studies[12–15] provide further support for the possibility of charge segregation and stripe correlations.

If the holes doped into an antiferromagnetic CuO_2 plane congregate in periodically spaced domain walls that separate antiphase magnetic domains, such correlations should be detectable by neutron diffraction. For example, the locally antiferromagnetic Cu spins are characterized by the two-dimensional wave vector $\mathbf{Q}_{AF}=(1/2,1/2)$ (where the components of **Q** are specified in units of $2\pi/a$). If the magnetic structure is modulated along the [100] direction with a period of n lattice spacings, then neutron diffraction should detect scattering not at $\mathbf{Q}_{AF}$, but instead at $(1/2\pm\epsilon,1/2)$, where $\epsilon=1/n$ [see Figs. 1(a) and 1(b)]. If a modulation along [010] is equally probable, then one should also find peaks at $(1/2,1/2\pm\epsilon)$. In fact, this is exactly what is observed[16–18] in superconducting crystals of $La_{2-x}Sr_xCuO_4$. The scattering is entirely inelastic, suggesting purely dynamical correlations; however, the experimentally determined periodicity differs from the Hartree-Fock prediction by a factor of 2, and this discrepancy led to an initial rejection[16] of the stripe-correlation picture. Instead, the split peaks observed by inelastic neutron scattering have commonly been interpreted in terms of a renormalized Fermi liquid with a nearly nested Fermi surface.[19–21]

Motivation to reconsider this issue has come from studies of stripe order[22–24] in the related nickelates, $La_2NiO_{4+\delta}$ and $La_{2-x}Sr_xNiO_4$. Following pioneering studies of magnetic correlations[25,26] and charge ordering[27] in nickelates with substantial hole doping, it was shown[22–24] that the magnetic and charge order are mutually commensurate, with the period of the spin modulation being twice that of the charge order, as expected for a striped phase. The direction of the modulation wave vectors indicates that the stripes run diagonally (i.e., along $\langle110\rangle$ directions) within a NiO_2 plane, in contrast to the vertical (and horizontal) stripes that are inferred in the cuprate case. The charge density in the hole stripes at low temperature (~1 per Ni site) is consistent with the multiband Hartree-Fock calculations of Zaanen and Littlewood;[28] however, in contrast to their model of holes ordering within an antiferromagnetic background, it is now clear that the ordering is driven by the charge, with the magnetic order

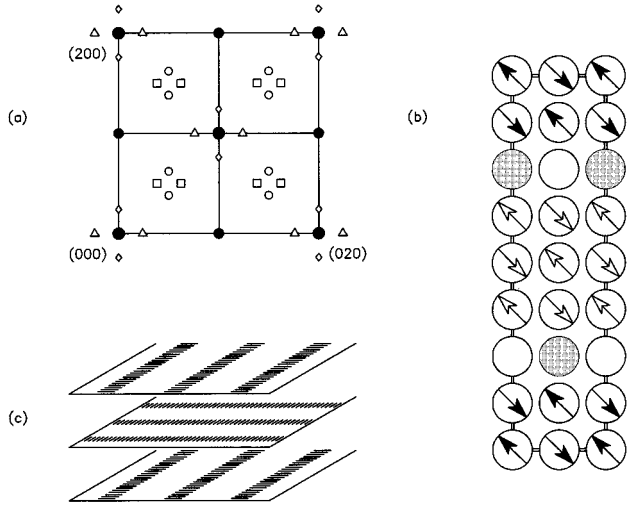

FIG. 1. (a) Diagram of the $(hk0)$ zone in reciprocal space. Large filled circles, fundamental Bragg peaks; small filled circles, superlattice peaks of the LTT phase. Open circles and squares, magnetic superlattice peaks from two different domains of the stripe structure; diamonds and triangles, charge-order superlattice peaks from the two stripe domains. Open circles and diamonds (squares and triangles) correspond to the same domain. (b) Model for the stripe order of holes and spins within a CuO_2 plane at $n_h = 1/8$. Only the Cu sites are represented. An arrow indicates the presence of a magnetic moment; shading of arrowheads distinguishes antiphase domains. A filled circle denotes the presence of one dopant-induced hole centered on a Cu site (hole weight is actually on oxygen neighbors). The charge order indicated within the stripes has not been observed, but serves as a reminder that the hole per Cu ratio is 1/2. A uniform hole density along the stripes is assumed in the analysis. (c) Sketch showing relative orientation of stripe patterns in neighboring planes of the LTT phase.

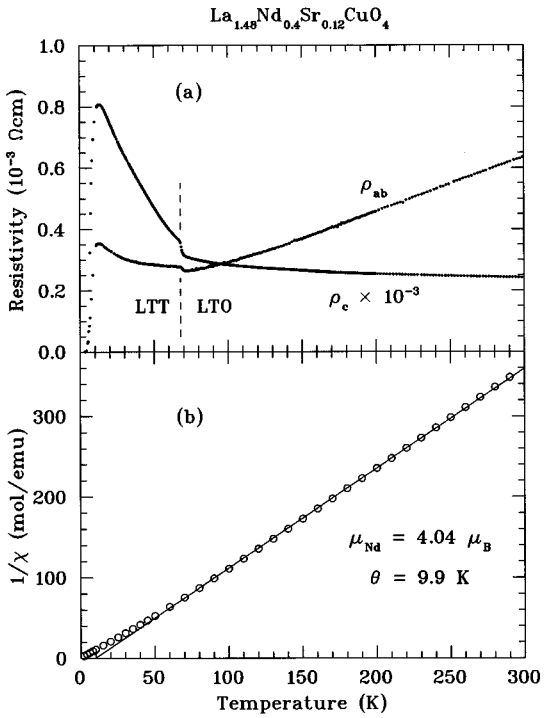

FIG. 2. (a) Resistivity measured parallel to the planes, ρ_{ab}, and perpendicular to them, ρ_c. Note that ρ_c is roughly 1000 time greater than ρ_{ab}. (b) Inverse of the bulk magnetic susceptibility vs temperature. Measurement was done in a 1 T field, with arbitrary sample orientation. Line through points is a Curie-Weiss fit, giving a net moment per Nd ion of $4.04\mu_B$ and $\theta = 9.9$ K.

following at a lower temperature.[29–31]

If stripe correlations are relevant to the cuprates, then one might hope to pin them, either with impurities or by an appropriate modulation of the lattice. One likely place to look for such effects is the $La_{2-x}Ba_xCuO_4$ system,[32,33] in which the superconducting transition temperature is anomalously depressed near $x \approx 1/8$. The anomaly in T_c is associated with a change in the lattice structure, from the usual low-temperature-orthorhombic (LTO) phase ($Bmab$ space group) to the low-temperature-tetragonal (LTT) phase ($P4_2/ncm$ space group).[34,35] Similar behavior is also found[36–38] in the system $La_{2-x-y}Nd_ySr_xCuO_4$.

We recently reported[39] neutron-diffraction evidence for both magnetic and charge order in the LTT phase of nonsuperconducting $La_{1.6-x}Nd_{0.4}Sr_xCuO_4$ with $x = 0.12$. In the present paper we describe new measurements on the original sample as well as on a second, newly grown crystal. After a brief description of the experimental procedures in the next section, the results are presented in Sec. III. There, in particular, we show scans of the temperature-dependent charge-order peaks at $(2 \pm 2\epsilon, 0, 0)$, and the absence of detectable signal at $(2, \pm 2\epsilon, 0)$, consistent with a longitudinal modulation of the lattice associated with the charge order. (Note that neutrons are directly sensitive only to the atomic displacements induced by the charge modulation.) The charge-order peaks appear at a higher temperature than the magnetic peaks, indicating that the stripe order is driven by the charge, rather than by the spins as one might expect if a magnetic Fermi-surface instability were involved. Below 3 K the magnetic intensity grows by an order of magnitude due to ordering of the Nd ions. From measurements of the diffuse scattering along $\mathbf{Q} = (1/2 - \epsilon, 1/2, l)$ we show that the magnetic order is quasi-two-dimensional (2D), with only weak correlations between second-nearest-neighbor layers. The implications of these results for the superconducting cuprates are discussed in Sec. IV.

II. SAMPLE CHARACTERIZATION AND EXPERIMENTAL DETAILS

The crystal used in the initial work was grown by Nakamura using the traveling-solvent floating-zone method; the transport properties measured on one piece of that crystal have been published elsewhere.[40] The in-plane and c-axis resistivities are reproduced in Fig. 2(a). One striking feature is that the in-plane resistivity measured in the LTO phase is nearly identical to that of a $La_{2-x}Sr_xCuO_4$ crystal with the same Sr concentration.[40] Although the resistivity rises somewhat as the temperature is lowered through the transition to the LTT phase near 70 K, it is still substantially lower at 10 K than at 300 K. (Below 10 K traces of superconductivity are apparent in the resistivity but not in the magnetization.) Figure 2(b) shows the inverse of the bulk magnetic susceptibility as a function of temperature measured on the second

crystal grown more recently by Ichikawa. As in the case[41] of Nd_2CuO_4, the susceptibility is dominated by the contribution from the Nd ions. A fit of the Curie-Weiss model to the data for $T>70$ K (line through data points) yields an effective moment of $(4.04\pm0.01)\mu_B$ and a paramagnetic Curie temperature of 9.9 K.

Each of the two crystals studied has a volume of ~ 0.1 cm^3 and a mosaic width of $\sim 0.2°$. At 10 K, in the LTT phase, the lattice parameters are $a=5.341$ Å and $c=13.08$ Å. Scattering measurements on the second crystal showed it to be essentially identical to the first crystal. Some of the results to be presented were measured on the first crystal and some on the second; because it makes no difference to the discussion, we will not bother to identify which crystal was used for each measurement.

The neutron-scattering experiments were performed on the triple-axis spectrometers H4M, H7, and H8 at the High Flux Beam Reactor at Brookhaven National Laboratory. In most of the measurements, 14.7 meV neutrons were selected using the (002) reflection of pyrolytic graphite (PG) for the monochromator and analyzer; in a few cases, such as the measurements of the magnetic form factor, an energy of 30.5 meV was used. Either one or two PG filters were placed in the incident beam to minimize the neutron flux at higher harmonic wavelengths. Relatively open horizontal collimation (40′-40′-80′-80′ from reactor to detector) was generally used; exceptions will be noted when appropriate.

Most of the measurements were performed in the $(h,k,0)$ zone ([001] perpendicular to the scattering plane), although some were carried out in the $(0.88h,h,l)$ zone. The samples were generally cooled with a Displex closed-cycle He refrigerator; in a few cases, a pumped ^{4}He cryostat was used. Temperatures were monitored with a Si diode in the former case, and a Ge sensor in the latter.

III. RESULTS

A. *Q* dependence

As we showed previously,[39] it is straightforward to observe the magnetic superlattice peaks at $(1/2\pm\epsilon,1/2,0)$ and $(\frac{1}{2},\frac{1}{2}\pm\epsilon,0)$ when the crystal is oriented in the $(h,k,0)$ zone; however, because of the quasi-2D nature of the scattering (to be discussed later), resolution effects have a dramatic effect on the visibility of the peaks. The collimation of a triple-axis spectrometer is generally relaxed in the vertical direction (perpendicular to the scattering plane), and the resolution width for the vertical component of the momentum transfer can easily be an order of magnitude greater than that for the in-plane components. Because the scattering of interest has only a small variation along [001] (at least for $T>5$ K), the poor vertical resolution provides an enhancement by integrating this signal when [001] is vertical, corresponding to the $(h,k,0)$ zone. This enhancement is lost when [001] is in the scattering plane. It seems likely that this resolution effect contributed to the lack of success in an earlier search for magnetic order in a similar crystal.[42]

Figure 3 shows scans of moderate resolution through the magnetic superlattice peaks at $(1/2\pm\epsilon,1/2,0)$ measured in the $(h,k,0)$ zone at 1.4 K, where the signal is further enhanced by the ordering of the Nd ions (to be discussed below). From these data we find that $\epsilon=0.118\pm0.001$. The

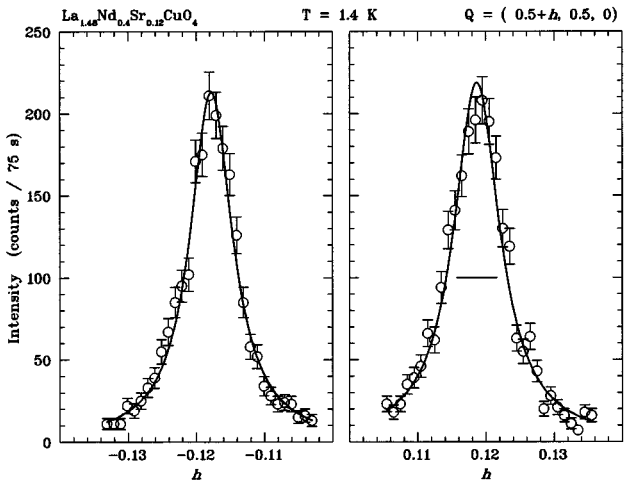

FIG. 3. Elastic scans through the magnetic superlattice peaks at $\mathbf{Q}=(1/2\pm\epsilon,1/2,0)$ obtained at $T=1.4$ K. Measured with horizontal collimations of 10′-40′-20′-40′ and a neutron energy of 14.7 meV. The lines through the data are fitted Lorentzians; the horizontal bar indicates the experimental resolution.

peak widths are slightly greater than resolution, and fits with a Lorentzian line shape yield an effective correlation length of ~ 170 Å along the modulation direction. Scans in the transverse direction give a similar correlation length parallel to the stripes.

Evidence for charge order is much more difficult to obtain, and we certainly would not have found any without a reasonable guess for where to look. Models of coupled charge and spin order predict that one should see charge-order-induced superlattice peaks split by $(\pm2\epsilon,0,0)$ about fundamental reciprocal lattice points such as (2,0,0). Figures 4(a) and 4(b) show scans through the position $(2\pm2\epsilon,0,0)$ at temperatures of 10 K and 65 K. We find structure in the scattering at both temperatures, with the temperature-dependent part of the signal considerably smaller than the background; nevertheless, when we subtract the 65 K data from the 10 K data, we find peaks, just slightly broader than resolution, at precisely the expected positions, as shown in Figs. 4(c) and 4(d). (Note that from the magnetic peak positions we expect that $2\epsilon=0.236$.) Besides the peaks, we also find a temperature-dependent background that must be taken into account in analyzing the variation of the peak intensity with temperature.

From the stripe-order model, peaks are also allowed at $(\pm2\epsilon,2,0)$, or, equivalently, at $(2,\pm2\epsilon,0)$. Scans through the latter positions are shown in Fig. 5. From the difference plots, Figs. 5(c) and 5(d), one finds that the peak intensity is negligible (i.e., it is at least an order of magnitude smaller than in Fig. 4). The difference between the measurements in Figs. 4 and 5 can be explained in terms of structure factors.

The atomic displacements that the neutrons detect are induced by the charge modulation via the corresponding electrostatic force, which should be proportional to the gradient of the electrostatic potential due to the charge stripes. Let **d** represent the magnitude and direction of the typical atomic displacement associated with the charge order; then we expect that

$$F(\mathbf{Q})\sim\mathbf{Q}\cdot\mathbf{d}, \tag{1}$$

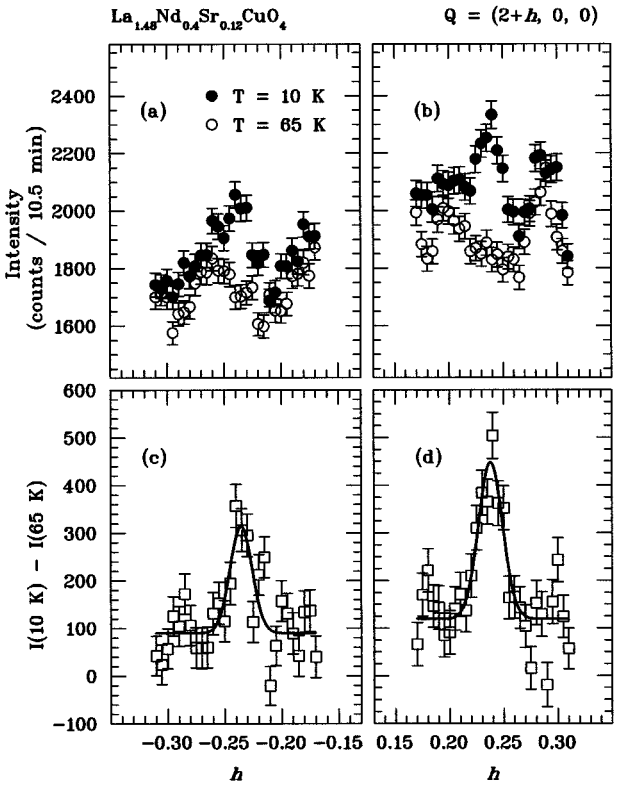

FIG. 4. (a) and (b) Elastic scans through the charge-order superlattice peaks at $\mathbf{Q}=(2\pm2\epsilon,0,0)$ at $T=10$ K (filled circles) and 65 K (open circles). (c) and (d) difference in intensity measured at 10 K and 65 K. Lines through the data are fitted Gaussians.

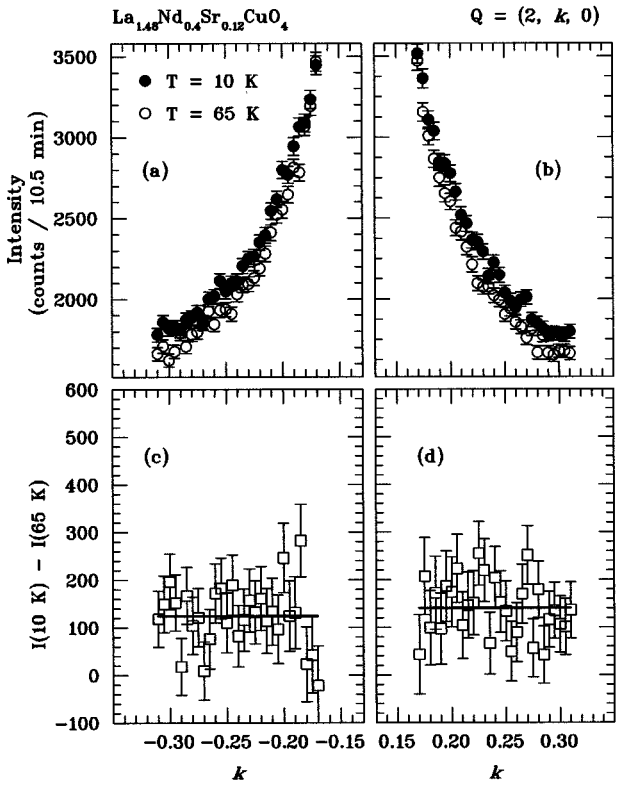

FIG. 5. Similar to the previous figure; here the scans are through the charge-order superlattice peak positions $\mathbf{Q}=(2,\pm\epsilon,0)$.

where F is the structure factor for the superlattice peak at wave vector $\mathbf{Q}$. The integrated peak intensity is proportional to $|F|^2$. For the stripe-order model, electrostatic considerations suggest that the displacements $\mathbf{d}$ should be predominantly along the modulation direction. It follows that

$$\frac{|F(2,2\epsilon,0)|^2}{|F(2+2\epsilon,0,0)|^2}\sim\frac{(2\epsilon)^2}{(2+2\epsilon)^2}=0.01, \tag{2}$$

consistent with experiment. Similarly, for the $(2\pm2\epsilon,0,0)$ peaks we expect

$$\frac{|F(2+2\epsilon,0,0)|^2}{|F(2-2\epsilon,0,0)|^2}\sim\frac{(2+2\epsilon)^2}{(2-2\epsilon)^2}=1.62, \tag{3}$$

while the experimental ratio is 2.1 ± 0.4, giving reasonable agreement.

B. *T* dependence

We have also studied the temperature dependence of the superlattice peak intensities. For the magnetic $(1/2-\epsilon,1/2,0)$ peak, the integrated intensity was initially determined by fitting to each scan a Gaussian plus a constant background. No significant temperature dependence of the background was found in these fits, so, to reduce fluctuations in the fitted peak areas associated with correlations between peak width and the background, the fits were repeated with the background fixed at its average value for all scans. The results, normalized at 10 K, are represented by the filled circles in Fig. 6.

Because of the low signal-to-background ratio for the charge-order peaks, we evaluated their integrated intensities in a simpler way, by just taking the area under the measured curve and subtracting the background determined from an

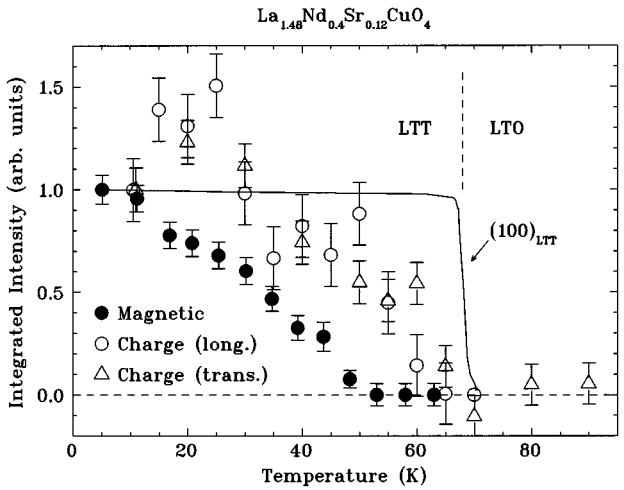

FIG. 6. Temperature dependence of the superlattice peak intensities, normalized at 10 K. Filled circles: magnetic peak at $(1/2-\epsilon,1/2,0)$; open circles: results for longitudinal scans through the charge-order peak at $(2+2\epsilon,0,0)$; open triangles: transverse scans through the same peak; solid line: (1,0,0) structural superlattice peak of the LTT phase.

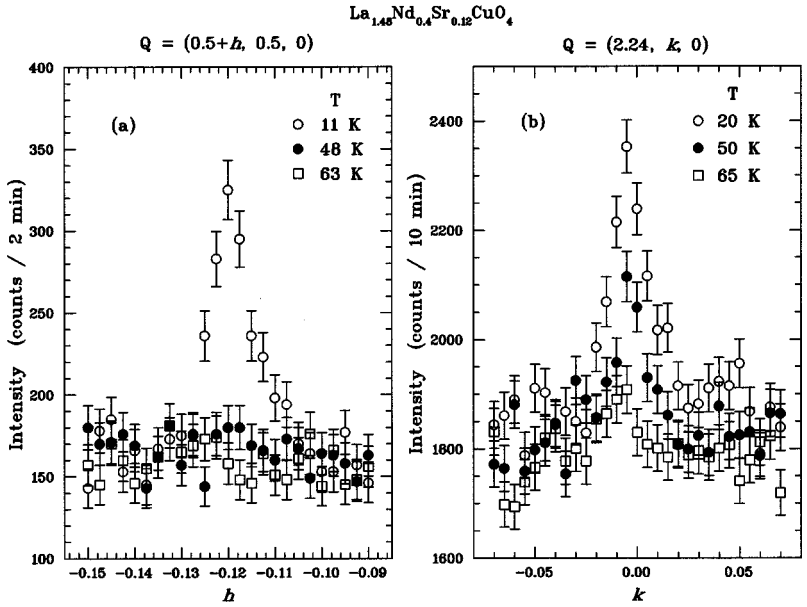

FIG. 7. (a) Scans through the $(1/2-\epsilon,1/2,0)$ magnetic peak at temperatures of 11, 48, and 63 K. (b) Transverse scans through the $(2+2\epsilon,0,0)$ charge-order peak at temperatures of 20, 50, and 65 K.

average of the regions to either side of each peak. The background was evaluated at each temperature, in order to take account of the temperature dependence of the background that is evident in Figs. 4 and 5; this was not properly accounted for in our initial study.[39] Data were collected for the $(2+2\epsilon,0,0)$ peak with scans performed both in the longitudinal direction along $(2+h,0,0)$, and in the transverse direction along $(2+2\epsilon,k,0)$. Because of structure in the nominal background, it is difficult to determine at what point the intensities of the charge peaks reach zero; hence, we have made the assumption that the average intensity in the LTO phase ($T \geqslant 70$ K) is zero. The results, normalized at 10 K, are shown in Fig. 6.

The most significant feature of the data concerns the different ordering temperatures for charge and spins: the charge orders at a higher temperature than the spins. To make this point clear, we compare in Fig. 7 scans of the magnetic and charge peaks at selected temperatures. [The temperatures in Fig. 7(b) do not identically match those in Fig. 7(a) because the measurements were made at different times with different cryostats (although on the same crystal).] As one can see, there is definitely a charge-order peak at 50 K, whereas there is no significant magnetic signal at 48 K. (The residual intensity in the charge peak scan at 65 K we believe to be an artifact.) These results indicate that the order is driven by the charge rather than the spins, as will be discussed below.

C. *l* dependence of magnetic scattering

Below 3 K the magnetic intensity grows rapidly, as illustrated in Fig. 8. This growth is due to ordering of the Nd moments and the development of weak correlations between next-nearest-neighbor layers. To study the Nd ordering and interlayer correlations, we measured the variation of the scattered intensity as a function of the momentum transfer perpendicular to the planes. Scans along $(1/2-\epsilon,1/2,l)$ at temperatures of 4.5 K and 1.38 K are plotted in Fig. 9. The broad diffuse scattering at 4.5 K becomes much more sharply peaked at 1.38 K, with strong features at $l=0$ and -3. (Note the change in counting time by a factor of 4.)

It is possible to explain the diffuse scattering with a simple model. We start with a single CuO_2 layer in which the Cu moments are ordered in antiferromagnetic stripes. Each Cu site has two La neighbors along the c axis, with apical oxygen atoms bridging the sites. 20% of the La sites are occupied by magnetic Nd ions. The orientation of each Nd moment is assumed to be correlated with its Cu neighbor. The l dependence of the magnetic scattering is then described by the structure factor (per Cu site)

$$\mathcal{F}_0(\mathbf{Q}) = \mathbf{p}_{\mathrm{Cu}} f_{\mathrm{Cu}}(\mathbf{Q}) + y\,\mathbf{p}_{\mathrm{Nd}} f_{\mathrm{Nd}}(Q)\cos(2\pi l z_{\mathrm{Nd}}), \qquad (4)$$

where $y=0.4$ (the Nd concentration per formula unit), z_{Nd} is the distance between a Nd and its Cu neighbor in units of c, f_{Cu} and f_{Nd} are magnetic form factors, and

$$\mathbf{p}_j = \boldsymbol{\mu}_j - \hat{\mathbf{Q}}(\hat{\mathbf{Q}}\cdot\boldsymbol{\mu}_j). \qquad (5)$$

In undoped La_2CuO_4, the spins lie along a [110] direction[43] as the result of competition between several very weak

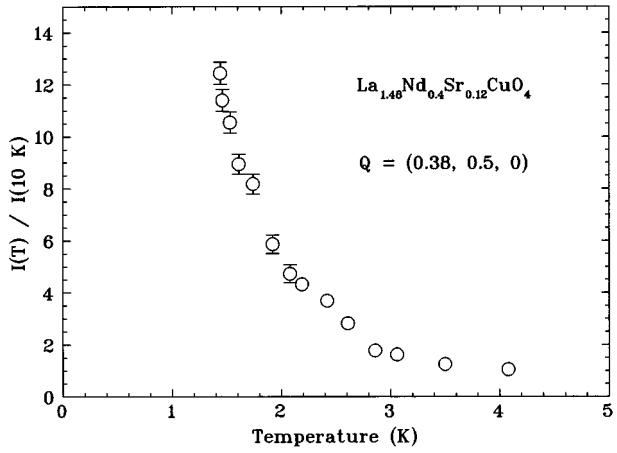

FIG. 8. Temperature dependence of the $(1/2-\epsilon,1/2,0)$ magnetic peak intensity below 5 K. The intensity is normalized to the value at 10 K.

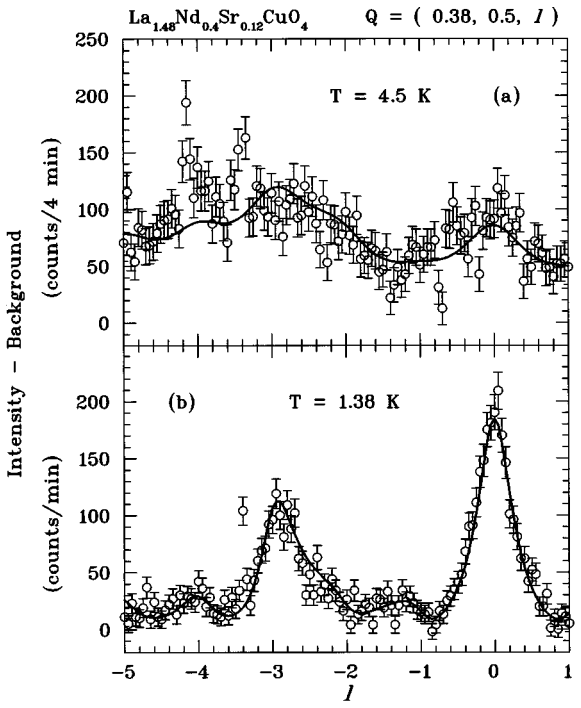

FIG. 9. Out-of-plane scans of the magnetic scattering along $\mathbf{Q}=(1/2-\epsilon,1/2,l)$ measured at temperatures of (a) 4.5 K and (b) 1.38 K. The background signal has been subtracted from the data. The lines through the data represent fits to a model discussed in the text. Note that the counting time for (a) is four times greater than for (b).

energies.[44] However, the rapid falloff of diffuse intensity in Fig. 9(b) as a function of $|l|$ indicates that the dominant contribution comes from spin components aligned along [001]. To take these points into account and simultaneously limit the number of fitting parameters, we allow for components of the Cu moment along **c** ($\mu_{\mathrm{Cu},\perp}$) and along [110] ($\mu_{\mathrm{Cu},\parallel}$), while the Nd moments are assumed to be completely along **c**. The scattered intensity should be proportional to $|\mathcal{F}_0|^2$, where, after averaging over possible domain structures, we have

$$|\mathcal{F}_0|^2=p_{\mathrm{Cu},\parallel}^2 f_{\mathrm{Cu}}^2+[p_{\mathrm{Cu},\perp}f_{\mathrm{Cu}}+yp_{\mathrm{Nd}}f_{\mathrm{Nd}}\cos(2\pi l z_{\mathrm{Nd}})]^2. \quad (6)$$

To quantitatively describe the structure observed at 1.38 K, it is also necessary to consider correlations between layers. We expect that correlations should only be possible between next-nearest-neighbor (NNN) layers, because the orientation of the antiferromagnetic stripes should rotate by 90° from one layer to the next [see Fig. 1(c)], following the structural distortion pattern of the LTT phase.[39] Correlations between NNN layers could be induced by pairs of bridging Nd ions. To describe correlations that decay exponentially with distance we make use of the formula[45,29]

$$|\mathcal{F}|^2=|\mathcal{F}_0|^2\frac{1-t^2}{1+t^2-2t\cos 2\pi l}, \quad (7)$$

where $t=\exp(-c/\xi)$.

To fit the data, theoretical magnetic form factors for Cu and Nd were used,[46,47] and the value of z_{Nd} (0.36) was taken from a neutron powder diffraction study.[33] The intensities calculated with Eqs. (6) and (7) were corrected for l-dependent resolution effects. Least-squares fits to the data are indicated by the solid lines in Fig. 9, and the parameter values obtained from the fits are listed in Table I.

TABLE I. Parameter values obtained in fitting the l-dependent diffuse magnetic scattering, as discussed in the text. Here $\mu_{\mathrm{Cu}}=(\mu_{\mathrm{Cu},\parallel}^2+\mu_{\mathrm{Cu},\perp}^2)^{1/2}$.

T	$\frac{\mu_{\mathrm{Cu}}(T)}{\mu_{\mathrm{Cu}}(1.38\mathrm{K})}$	$\frac{\mu_{\mathrm{Cu},\perp}}{\mu_{\mathrm{Cu},\parallel}}$	$\frac{\mu_{\mathrm{Nd}}}{\mu_{\mathrm{Cu}}}$	$\frac{\xi}{c}$
1.38 K	1.0	0.97±0.07	3.9±0.4	0.55±0.07
4.5 K	1.1±0.2	0.37±0.07	0.5±0.1	0.28±0.17

Looking at Table I, we see that, while the net Cu moment shows essentially no change, the ordered Nd moment grows by a factor of 8 on cooling from 4.5 to 1.38 K. As the Nd moment grows, the Cu spins (on average) rotate out of the plane, and interplanar correlations grow. While the temperature dependence of the magnetic scattering shown in Fig. 8 suggests that most of the Nd ordering occurs below 3 K, it is interesting to note that the Nd moment is still finite at 4.5 K.

D. Effective magnetic form factor

As another check on the magnetic scattering, we measured the integrated intensities for a number of $(hk0)$-type magnetic reflections at a temperature of 1.4 K using 30.5 meV neutrons. For the model of magnetic order discussed above, we can extract from the structure factors an effective magnetic form factor given by

$$f_{\mathrm{eff}}=\left[\frac{\frac{1}{2}\mu_{\mathrm{Cu},\parallel}^2 f_{\mathrm{Cu}}^2+(\mu_{\mathrm{Cu},\perp}f_{\mathrm{Cu}}+y\mu_{\mathrm{Nd}}f_{\mathrm{Nd}})^2}{\frac{1}{2}\mu_{\mathrm{Cu},\parallel}^2+(\mu_{\mathrm{Cu},\perp}+y\mu_{\mathrm{Nd}})^2}\right]^{1/2}. \quad (8)$$

The solid line in Fig. 10 shows the effective form factor calculated using the theoretical form factors and the experimentally determined moment ratios from Table I (1.38 K

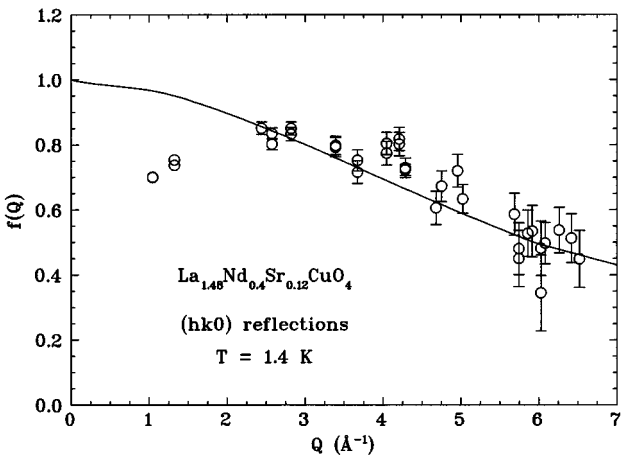

FIG. 10. Structure factors of the magnetic $(hk0)$ reflections measured at $T=1.4$ K (circles) normalized to the calculated effective magnetic form factor (line).

results). The circles with error bars indicate the values obtained from the measured structure factors, normalized to the calculation. The data and the calculation are reasonably consistent for $Q>2$ Å^{-1}. The deviation at small Q might indicate that there is some net spin density on O sites. The form factor for O falls off much more rapidly with Q than those for Cu and Nd, and if the O spin density is antiparallel to the Cu and Nd, the O contribution would subtract from the net Cu-plus-Nd form factor. A net spin density might be induced on an apical oxygen site bridging Cu and Nd sites.

We have assumed to this point that the component of the Cu spin in the plane is along a [110] direction. It is possible that the in-plane component could lie along a different direction. For example, in antiferromagnetic $La_{1.65}Nd_{0.35}CuO_4$ the spin direction is along [110] when the crystal has the LTO structure, but below 76 K, where the space group changes to $Pccn$, it has been argued that the spins may rotate towards a [100] or [010] direction.[42,48] (Note that there is also evidence[42] for a canting of the Cu spins that results in a net ferromagnetic moment in the low-temperature phase, with a possible Nd contribution below ~20 K.) In our previous paper,[39] we drew a diagram of the stripe order suggesting a spin direction transverse to the direction of the charge modulation, by analogy with the nickelate case; however, putting the in-plane component along [100] or [010] results in a substantial modulation of the effective form factor as a function of **Q** that is incompatible with the data.

E. Size of the ordered Cu moment

The average ordered Cu moment, μ_{Cu}, can be evaluated directly from the intensity of the magnetic scattering. For this purpose, we have used the integrated intensities of magnetic $(hk0)$ peaks measured at 1.4 K that were discussed above. The structure factors extracted from the intensities should correspond to

$$|F|^2=\frac{1}{4}A\left(\frac{r_0}{2\mu_B}\right)^2|2\mathcal{F}|^2, \tag{9}$$

where A is a scale factor dependent on sample volume, r_0 is equal to 0.539×10^{-12} cm, and $|2\mathcal{F}|^2$ is given by Eqs. (6) and (7), with an extra factor of 2 included to account for two Cu atoms per plane within an LTT unit cell. The factor A is determined from a fit to measured intensities for seven fundamental nuclear Bragg peaks, allowing for extinction (which is substantial for the strongest peaks).[49] One complication is that the nuclear peaks are true Bragg peaks, while the magnetic scattering is extended along l. To take account of this, we have multiplied the l-dependent line-shape function in Eq. (7) by the known vertical resolution function and integrated; using the result, we make the replacement

$$|2\mathcal{F}|^2\rightarrow0.5|2\mathcal{F}_0|^2. \tag{10}$$

For the form factors in Eq. (6), we use values consistent with the normalization shown in Fig. 10; the other parameters are taken from Table I. Putting all of the numbers together, we find $\mu_{\mathrm{Cu}}=0.10\pm0.03\mu_B$.

Our measurement of the average ordered moment μ_{Cu} only provides a lower limit for the local moment $\tilde{\mu}_{\mathrm{Cu}}$ on an individual Cu site. Fluctuations of the spin direction, which one might expect to be important in the present case of quasi-2D order, would reduce the average moment compared to the local value. This effect can be expressed as $\mu_{\mathrm{Cu}}=f\tilde{\mu}_{\mathrm{Cu}}$ with $0<f<1$. An alternative way to measure $\tilde{\mu}_{\mathrm{Cu}}$ is to compare it with the Nd moment. For Nd we expect that $\mu_{\mathrm{Nd}}=f'\tilde{\mu}_{\mathrm{Nd}}$ with $f'\leqslant f$. The factor f' for Nd can be no greater than the factor f for Cu because each Nd can order only through its interaction with Cu moments. From these relationships, one finds that

$$\tilde{\mu}_{\mathrm{Cu}}=\frac{f'}{f}\frac{\mu_{\mathrm{Cu}}}{\mu_{\mathrm{Nd}}}\tilde{\mu}_{\mathrm{Nd}}. \tag{11}$$

The ratio $\mu_{\mathrm{Nd}}/\mu_{\mathrm{Cu}}$ has already been determined experimentally from the l dependence of the magnetic scattering, and the local Nd moment can be estimated from the susceptibility measurements. If the orientation of each Nd spin was perfectly correlated with the nearest-neighbor Cu spin, then we would have $f'/f=1$ and could directly evaluate $\tilde{\mu}_{\mathrm{Cu}}$. It is unlikely that we reached such a state of perfect correlation in our experiment, since the intensity of the magnetic scattering had not saturated at the lowest measurement temperature; nevertheless, we can determine an upper limit for the local Cu moment by using Eq. (11) and setting $f'/f=1$.

The effective Nd moment of $4.04\mu_B$ obtained from the Curie-Weiss fit to the susceptibility corresponds to

$$\mu_{\mathrm{Nd}}^{\mathrm{eff}}=\langle\tilde{\mu}_{\mathrm{Nd}}^2\rangle^{1/2}=g\sqrt{J(J+1)}\mu_B, \tag{12}$$

whereas the local moment should correspond to $\tilde{\mu}_{\mathrm{Nd}}=gJ\mu_B$. Scaling the effective moment by $\sqrt{J/(J+1)}$, with $J=9/2$, gives $\tilde{\mu}_{\mathrm{Nd}}\approx3.7\mu_B$. Combining this with the 1.38 K result $\mu_{\mathrm{Nd}}/\mu_{\mathrm{Cu}}=3.9$ (see Table I), we get the upper limit $\tilde{\mu}_{\mathrm{Cu}}=0.95\mu_B$, which is essentially the full moment for an $S=1/2$ ion.

IV. DISCUSSION

A. Magnetic order

The elastic neutron-diffraction peaks at positions of the type $(1/2\pm\epsilon,1/2,0)$ provide clear evidence of magnetic order in the CuO_2 planes below ~50 K in the LTT phase. Analysis of the intensities of $(hk0)$ reflections yields an effective form factor with a Q dependence that is consistent with magnetic scattering. The ordering of the Nd moments at low temperature provides a useful confirmation of the nature of the order. The Nd ions by themselves are too dilute to drive magnetic order, let alone an incommensurate ordering; however, by following their Cu neighbors they are able to amplify the magnetic signal.

In representing the magnetic order in Fig. 1(b) we have assumed that it is the amplitude of the spin density that it is modulated. Alternatively, it is possible in principle that the spin density might be constant while the direction of the spin is modulated. In particular, one could imagine the orientation of the spins rotating from one row to the next along the modulation direction, thus yielding a spiral order. Spiral phases of the doped antiferromagnetic planes were originally proposed for the cuprates based on mean-field analyses of the t-J model.[50,51] It has since been shown that the spiral

phase is unstable towards the formation of an inhomogeneous state involving charged domain walls.[52–54] (The domain walls are a form of phase separation, a tendency for which had previously been predicted.[55,56]) Despite theoretical difficulties with spiral order, it is worthwhile to consider whether it is possible to distinguish experimentally between a density modulation and an orientation modulation.

In the case of stripe order in $La_2NiO_{4.125}$, it was possible to rule out a spiral modulation based on an analysis of magnetic peak intensities.[24] The diagonal orientation of the stripes made it possible to show that the spins are all aligned transverse to the modulation direction. Unfortunately, the $\langle 100 \rangle$ modulation directions prevent one from making such a distinction in the cuprate. We can, nevertheless, draw a partial conclusion based on the ordering of the Nd moments. At 4.5 K and above, the Cu spins lie close to the CuO_2 planes. If the magnetic modulation involved a spiral of the in-plane spin components, then all Nd ions would see the same local field, and hence the c-axis-oriented Nd moments would never couple to the modulation. The fact that the Nd moments *do* couple to the magnetic modulation is proof that the order is not an in-plane spiral. We cannot, however, rule out a spiral with an out-of-plane component (although we consider it unlikely).

Although the magnetic scattering consists of sharp peaks in the $(hk0)$ zone, it is diffuse along l, indicating that the order is quasi-2D. Our analysis indicates that the maximum ordered Cu moment is $0.10\mu_B$, 20% of the moment found in three-dimensionally ordered La_2CuO_4. If the Cu moments are considered to have a Heisenberg coupling, then, given the quasi-2D nature of the order and the importance of zero-point spin fluctuations, one may consider the observed moment to be rather substantial. On the other hand, the Nd moments may provide an important source of anisotropy necessary to allow static 2D spin order, and the significance of this anisotropy for limiting Cu spin fluctuations is not known.

Another measure of the magnetic moment is given by muon spin-rotation (μSR) spectroscopy. Recent measurements[57] on one of the $La_{1.48}Nd_{0.4}Sr_{0.12}CuO_4$ crystals indicate an average hyperfine field comparable to that measured[58] in $La_{1.875}Ba_{0.125}CuO_4$, and about 80% of the field observed[59,60] in stoichiometric La_2CuO_4. Assuming that the muons sit at similar sites in all of these compounds, the μSR results imply a local ordered moment of $\sim 0.4\mu_B$. [Note that the observation of a larger moment by μSR (a local probe) than that found by neutron diffraction (which averages over the entire sample) is consistent with the trend found[59,60] in weakly doped La_2CuO_4.] Such a large moment would be difficult to explain starting from a weak-coupling spin-density-wave model.

B. Charge order

The observation of superlattice peaks at $(2 \pm 2\epsilon,0,0)$ demonstrates that there is a modulation of the lattice that is coupled to the magnetic order. Although their intensities are extremely weak, the peaks appear at precisely the expected positions, and exhibit a reasonable temperature dependence. If 2ϵ were equal to 0.25, then, ignoring the temperature dependence of the intensities, one might be tempted to attribute the observed peaks to scattering by neutrons with $\lambda/4$. The fact that $2\epsilon = 0.236$ rules out this possibility. We believe that the observed peaks are direct evidence for charge order.

To be consistent with the magnetic scattering, the charge-order correlations should be two dimensional. So far we have only indirect evidence for this: the $(2 \pm 2\epsilon,0,0)$ peaks are detectable in the $(hk0)$ zone, but not when we rotate the crystal so that $\mathbf{c}^*$ is in the scattering plane. For 2D correlations, the scattering should be independent of l, and in the $(hk0)$ zone $[00l]$ is in the vertical direction. The momentum resolution in the vertical direction is an order of magnitude more coarse than in the horizontal plane, which allows an effective partial integration of the 2D scattering in the $(hk0)$ configuration that is lost when $\mathbf{c}^*$ is rotated into the horizontal plane.

A proper analysis of the atomic displacements associated with the charge order would require experimental structure factors for many more superlattice peaks; nevertheless, we can make a rough estimate of the magnitude of the displacements implied by our observations. Let us assume that the displacements involve only breathing motions of the in-plane oxygens, and that their motion is parallel to the modulation wave vector. Then, if the magnitude of the displacement wave (in Å^{-1}) is denoted by Δr_O, we find that

$$\frac{|F(2+2\epsilon,0,0)|^2}{|F(2,0,0)|^2} = 0.081(\Delta r_O)^2. \tag{13}$$

To obtain an experimental ratio, it is necessary to correct the (2,0,0) intensity for substantial extinction, and to account for the partial integration of the 2D charge-order scattering; doing so, we obtain

$$\frac{|F(2+2\epsilon,0,0)|^2}{|F(2,0,0)|^2} = (1.6 \pm 0.3) \times 10^{-6}. \tag{14}$$

The estimated magnitude of the O displacements is then $\Delta r_O \approx 0.004$ Å. This value may be compared with $\Delta r_O = 0.018$ Å found[24] in $La_2NiO_{4.125}$. The smaller displacement in the cuprate is consistent with the lower charge density in the hole stripes compared to the nickelate and with the theoretical expectation[28] of a weaker electron-phonon coupling than in the nickelates.

It is not possible to directly obtain the degree of charge modulation from the estimated displacement. We can gain some perspective on the problem, though, by comparing with the change in the Cu-O bond length in $La_{2-x}Sr_xCuO_4$ due to doping. On changing x from 0 to 0.15, r_{Cu-O} is found[61,62] to decrease by 0.016 Å. If the stripe phase consists of hole-rich and hole-poor domains, then one might expect $\Delta r_O \sim \Delta r_{Cu-O}$, and we find this to be roughly the case.

The observation that the charge ordering occurs at a higher temperature than the spin ordering says a great deal about the driving force for the order. Using a simple Ginzburg-Landau free-energy argument involving the charge and magnetization densities, Emery and Kivelson[63] have shown that there are two possible scenarios. If the magneti-

zation density orders first, then the charge density will follow at the same temperature, with the charge order parameter varying as the square of the magnetization. This situation describes chromium.[64] Alternatively, if the charge density orders first, then the magnetization need not order at the same temperature, as we observe in the cuprate.

Charge-driven order is not consistent with the standard proposals for an instability associated with the Fermi surface. In the renormalized-Fermi-liquid scenario, one would expect the spin susceptibility to diverge first. Instead, it appears that the holes segregate first, which results in hole-free domains that allow for local antiferromagnetic order at a lower temperature. It is now clear that the stripe-phase order in $La_2NiO_{4+\delta}$ and $La_{2-x}Sr_xNiO_4$ is also charge driven.[29–31]

One feature of the stripe order that we have not discussed is the shape of the domain walls. The superlattice peaks that we have observed only provide information about the first Fourier component of the charge and spin densities. Possible deviations from a sinusoidal modulation must be determined from higher harmonics. A quantitative analysis of such higher harmonics has been performed for the case of stripe order in $La_2NiO_{4+\delta}$, where it is found that sharp domain walls result in very weak harmonics (on the order of 1% of the first harmonic).[30] Detecting higher harmonics will be a much greater challenge in the cuprates.

Given the weakness of the charge-order peaks, it is certainly desirable to characterize them with other techniques, such as electron and x-ray diffraction. Electron-diffraction studies so far have been unsuccessful in detecting the peaks.[65] Electron scattering should certainly be sensitive to charge ordering; however, before one jumps to any hasty conclusions, it is worthwhile to consider the detection problem quantitatively. With neutrons, we find that the intensities of the charge-order peaks, relative to fundamental reflections, are more than 200 times weaker than the strongest charge-order peak observed[24] in $La_2NiO_{4.125}$. Detection requires careful attention to minimizing background and taking advantage of the temperature dependence of the signal. In the nickelate, the oxygens undergo the largest displacements, and we expect the same to be true in the cuprate. Neutrons, which scatter from nuclei, have comparable sensitivity to all of the elements in both compounds, whereas the scattering of electrons and x rays is dominated by the high-Z elements. Thus, one does not automatically gain sensitivity by using a technique that scatters from the electron density.

Before concluding this section, it seems worthwhile to comment on recent reports of $(\frac{1}{2}\ \frac{1}{2}\ 0)$-type superlattice reflections in electron-[66] and x-ray-[67] diffraction studies of $La_{2-x}Ba_xCuO_4$ and $La_{2-x}Sr_xCuO_4$. In one case, the observation of such peaks was interpreted as evidence for a charge-density wave.[66] We have also observed surprisingly strong scattering at $(\frac{1}{2}\ \frac{1}{2}\ 0)$; however, we were able to essentially eliminate all of the signal at this point by tuning the neutron wavelength. [An example of a scan through $(\frac{1}{2}\ \frac{1}{2}\ 0)$ made after tuning the wavelength is shown in Fig. 3(b) of Ref. 39.] The dramatic sensitivity of the scattered intensity to the wavelength indicates that the reflection (in our case, at least) is due to multiple scattering. The likelihood that multiple scattering is important in the other studies should be carefully considered.

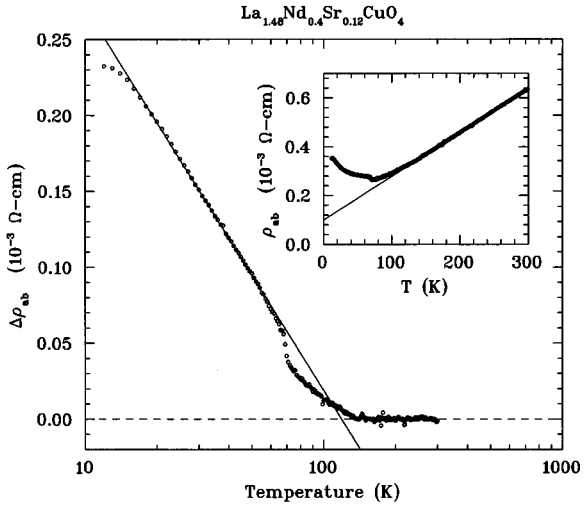

FIG. 11. In-plane resistivity data (points), after subtracting linear fit to $T>150$ K data, plotted vs ln$T$. The solid line indicates $\ln(T_0/T)$ behavior. Inset: Original data, showing linear fit and extrapolation (solid line).

C. Resistivity

One would expect charge segregation and ordering to have a substantial impact on the electrical resistivity. Thus, it is of interest to reexamine the resistivity data in light of the diffraction results. To do so, we have attempted to fit the temperature dependence of the resistivity in the LTO phase with simple functional forms. For the in-plane resistivity, data corresponding to $T>150$ K were fit to the form

$$\rho_{ab}(\mathrm{LTO}) = a + bT, \tag{15}$$

as indicated in the inset of Fig. 11. After extrapolating the curve to low temperature and subtracting from the raw data, we get the difference shown in the main panel of Fig. 11. Note that the resistivity in the LTO phase begins to deviate from linearity below 140 K, and the steplike jump near 70 K corresponds to the structural transition. Surprisingly, we find that the resistivity in the LTT phase is fit rather well by

$$\Delta\rho_{ab} \equiv \rho_{ab} - (a + bT) = c + \ln(T_0/T). \tag{16}$$

The deviation below 15 K is associated with the residual superconductivity. The $\ln(T_0/T)$ behavior is reminiscent of the low-temperature normal-state resistivities found in $La_{2-x}Sr_xCuO_4$ by Ando *et al.*[68] when the superconductivity is suppressed by application of a 61 T magnetic field. In the present case, we believe that superconductivity is suppressed due to pinning of the stripe-phase charge and spin correlations due to the LTT distortion. The details of ρ_{ab} should not be over interpreted because ρ_{ab} measured on Ishikawa's crystal shows some quantitative difference from Nakamura's. The most significant observation is the lack of any sign of the charge-ordering transition. A proper comparison with the findings of Ando *et al.*[68] requires measurements in a

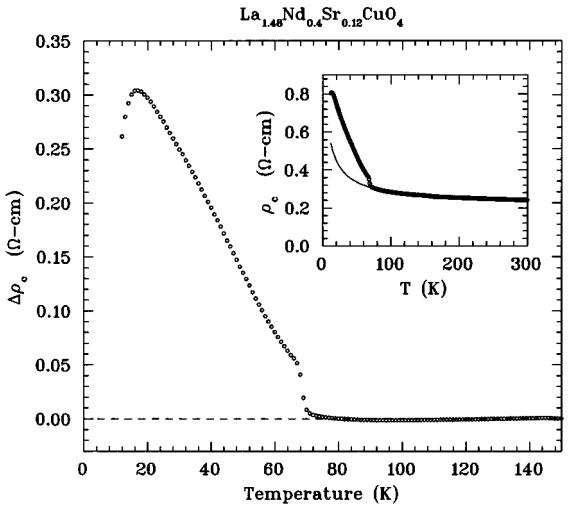

FIG. 12. Resistivity along the c axis, after subtracting $d+\ln(T_0'/T)/T$ contribution fit to LTO regime. Inset: Original data (points) and fit to the LTO regime (solid line).

magnetic field, and the results of such measurements will be reported in the near future.[69]

For the out-of-plane resistivity, we fit the LTO data to the function

$$\rho_c(\mathrm{LTO}) = d + \frac{\ln(T_0'/T)}{T}, \tag{17}$$

as shown in the inset of Fig. 12. Subtracting the extrapolated fit from the data gives the points shown in the main panel of Fig. 12. In the LTT phase, below the jump at ~ 70 K, the behavior of $\Delta\rho_c$ has some similarity to the temperature dependence of the charge order parameter shown in Fig. 6. Further work is required to establish a clear connection between $\Delta\rho_c$ and the charge ordering; nevertheless, the greater sensitivity of ρ_c to correlations within the planes has also been seen in $YBa_2Cu_3O_{7-y}$ in association with the ''spin-gap'' behavior.[70]

D. Significance

The observation of stripe order in $La_{1.48}Nd_{0.4}Sr_{0.12}CuO_4$ is important because of its connection with the inelastic magnetic scattering found[16–18] in $La_{2-x}Sr_xCuO_4$. The Q dependence of the magnetic scattering in the two systems is essentially identical. While the corresponding charge correlations are not directly evident in the metallic cuprates, we have provided evidence that the magnetic correlations in the Nd-doped compound are the result of charge segregation. We suggest that the only difference between the charge and spin correlations in these various compounds is that they can become pinned to the lattice in the LTT structure, whereas they remain purely dynamical in the LTO phase. The pinning in the LTT phase is easily rationalized. The pattern of tilts of the CuO_6 octahedra within the CuO_2 planes of the LTO structure forms diagonal stripes, whereas the tilt pattern in the LTT phase consists of horizontal stripes that rotate by 90° on going from one layer to the next. (Besides the tilt modulation, there is also a difference in Cu-O bond lengths along orthogonal directions within the CuO_2 planes in the LTT phase.[71]) The horizontal lattice-distortion pattern in the latter case is oriented parallel to the charge stripes. If the period of the charge stripes is commensurate with the lattice distortion, then one expects pinning.

The observed value of the peak splitting parameter, $\epsilon = 0.118 \pm 0.001$, is quite close to the commensurate value of 1/8. The difference can be attributed to discommensurations. If we consider a model with narrow charge stripes, then the pattern of discommensurations can be understood in a simple way. For the model structure shown in Fig. 1(b) corresponding to $\epsilon = 1/8$, the spacing between charge stripes is $4a$; however, if every fourth spacing is reduced from $4a$ to $3a$, then the corresponding value of ϵ is 0.1176.

Pinning of the charge and spin stripes in the LTT phase is associated with the suppression of superconductivity. Büchner *et al.*[37] have found a rather intriguing competition between superconductivity and the LTT phase in $La_{1.85-y}Nd_ySr_{0.15}CuO_4$. Could this indicate, indirectly, a competition between superconducting and stripe-ordered ground states? The magnetoresistance measurements on $La_{2-x}Sr_xCuO_4$ by Ando *et al.*,[68] in which an ''insulating'' phase is obtained when superconductivity is suppressed with a magnetic field, lend encouragement to such speculations. Such a possibility deserves further investigation.

Dynamical charge segregation with a stripe morphology is clearly a type of correlation that must be taken into account before transport properties can be understood. Stripe correlations may be responsible for the lack of resistivity saturation at high temperatures, a feature that is not compatible with quasiparticle transport.[72,73] Several studies have begun to address the problem of stripe dynamics[74,75] and the effect of phase separation instabilites on charge scattering.[13] It has been shown[76] that the photoemission features calculated for a model of disordered stripes (intended to represent slowly fluctuating stripes) is consistent with experiments on $Bi_2Sr_2CaCu_2O_{8+\delta}$. A stripe-phase model has also been used[77,78] to model the decrease of magnetization and Néel temperature with doping for small x in $La_{2-x}Sr_xCuO_4$.

Many of the analyses mentioned in the previous paragraph take a charge-stripe phase as a starting point. There still remain questions concerning the observed charge density (one hole per two Cu sites) within the stripes. Zaanen and Oleś[15] have recently shown that for such a density to be explained by a Hartree-Fock treatment of the Hubbard model there must be a quadrupling (as opposed to a doubling) of the period along the stripes. Such a model predicts extra superlattice peaks that should be rather weak. Experimentally, a careful search for the predicted peaks has not yet been performed. Alternatively, inclusion of quantum fluctuations and/or the long-range part of the Coulomb interaction may be necessary.[9,13]

ACKNOWLEDGMENTS

Valuable discussions with V. J. Emery, S. A. Kivelson, J. P. Sethna, and B. J. Sternlieb are gratefully acknowledged. Work at Brookhaven was carried out under Contract No. DE-AC02-76CH00016, Division of Materials Sciences, U.S. Department of Energy.

[1] J. Zaanen and O. Gunnarsson, Phys. Rev. B **40**, 7391 (1989).
[2] H. J. Schulz, J. Phys. (Paris) **50**, 2833 (1989).
[3] D. Poilblanc and T. M. Rice, Phys. Rev. B **39**, 9749 (1989).
[4] M. Kato, K. Machida, H. Nakanishi, and M. Fujita, J. Phys. Soc. Jpn. **59**, 1047 (1990).
[5] J. A. Vergés *et al.*, Phys. Rev. B **43**, 6099 (1991).
[6] M. Inui and P. B. Littlewood, Phys. Rev. B **44**, 4415 (1991).
[7] T. Giamarchi and C. Lhuillier, Phys. Rev. B **42**, 10 641 (1990).
[8] G. An and J. M. J. van Leeuwen, Phys. Rev. B **44**, 9410 (1991).
[9] V. J. Emery and S. A. Kivelson, Physica C **209**, 597 (1993).
[10] U. Löw, V. J. Emery, K. Fabricius, and S. A. Kivelson, Phys. Rev. Lett. **72**, 1918 (1994).
[11] S. A. Kivelson and V. J. Emery, in *Strongly Correlated Electronic Materials: The Los Alamos Symposium 1993*, edited by K. S. Bedell *et al.* (Addison-Wesley, Reading, MA, 1994), pp. 619–656.
[12] S. Haas, E. Dagotto, A. Nazarenko, and J. Riera, Phys. Rev. B **51**, 5989 (1995).
[13] C. Castellani, C. D. Castro, and M. Grilli, Phys. Rev. Lett. **75**, 4650 (1995).
[14] L. Chayes *et al.*, Physica A **225**, 129 (1996).
[15] J. Zaanen and A. M. Oleś, Ann. Phys. (Leipzig) **5**, 224 (1996).
[16] S.-W. Cheong *et al.*, Phys. Rev. Lett. **67**, 1791 (1991).
[17] T. E. Mason, G. Aeppli, and H. A. Mook, Phys. Rev. Lett. **68**, 1414 (1992).
[18] T. R. Thurston *et al.*, Phys. Rev. B **46**, 9128 (1992).
[19] N. Bulut, D. Hone, D. J. Scalapino, and N. E. Bickers, Phys. Rev. Lett. **64**, 2723 (1990).
[20] J. P. Lu, Q. Si, J. H. Kim, and K. Levin, Phys. Rev. Lett. **65**, 2466 (1990).
[21] P. B. Littlewood, J. Zaanen, G. Aeppli, and H. Monien, Phys. Rev. B **48**, 487 (1993).
[22] J. M. Tranquada, D. J. Buttrey, V. Sachan, and J. E. Lorenzo, Phys. Rev. Lett. **73**, 1003 (1994).
[23] V. Sachan *et al.*, Phys. Rev. B **51**, 12 742 (1995).
[24] J. M. Tranquada, J. E. Lorenzo, D. J. Buttrey, and V. Sachan, Phys. Rev. B **52**, 3581 (1995).
[25] S. M. Hayden *et al.*, Phys. Rev. Lett. **68**, 1061 (1992).
[26] K. Yamada *et al.*, Physica C **221**, 355 (1994).
[27] C. H. Chen, S.-W. Cheong, and A. S. Cooper, Phys. Rev. Lett. **71**, 2461 (1993).
[28] J. Zaanen and P. B. Littlewood, Phys. Rev. B **50**, 7222 (1994).
[29] J. M. Tranquada, D. J. Buttrey, and V. Sachan (unpublished).
[30] P. Wochner, J. M. Tranquada, D. J. Buttrey, and V. Sachan (unpublished).
[31] A. P. Ramirez *et al.*, Phys. Rev. Lett. **76**, 447 (1996).
[32] A. R. Moodenbaugh *et al.*, Phys. Rev. B **38**, 4596 (1988).
[33] J. D. Axe and M. K. Crawford, J. Low Temp. Phys. **95**, 271 (1994).
[34] J. D. Axe *et al.*, Phys. Rev. Lett. **62**, 2751 (1989).
[35] Y. Zhu *et al.*, Phys. Rev. Lett. **73**, 3026 (1994).
[36] M. K. Crawford *et al.*, Phys. Rev. B **44**, 7749 (1991).
[37] B. Büchner *et al.*, Europhys. Lett. **21**, 953 (1993).
[38] B. Büchner, M. Breuer, A. Freimuth, and A. P. Kampf, Phys. Rev. Lett. **73**, 1841 (1994).
[39] J. M. Tranquada *et al.*, Nature **375**, 561 (1995).
[40] Y. Nakamura and S. Uchida, Phys. Rev. B **46**, 5841 (1992).
[41] M. F. Hundley *et al.*, Physica C **158**, 102 (1989).
[42] S. Shamoto *et al.*, Physica C **203**, 7 (1992).
[43] D. Vaknin *et al.*, Phys. Rev. Lett. **58**, 2802 (1987).
[44] T. Yildirim, A. B. Harris, O. Entin-Wohlman, and A. Aharony, Phys. Rev. Lett. **72**, 3710 (1994).
[45] A. Guinier, *X-Ray Diffraction in Crystals, Imperfect Crystals, and Amorphous Bodies* (Dover, New York, 1994).
[46] S. Shamoto *et al.*, Phys. Rev. B **48**, 13 817 (1993).
[47] M. Blume, A. J. Freeman, and R. E. Watson, J. Chem. Phys. **37**, 1245 (1962).
[48] B. Keimer *et al.*, Z. Phys. B **91**, 373 (1993).
[49] Measurement of the nuclear peak intensities required the use of an attenuator. Measurements performed after the original submission of this paper showed that we had underestimated the net attenuation factor by 40%. Correcting for this systematic error increases the scale factor A and reduces the value of μ_{Cu} relative to our original result.
[50] B. I. Shraiman and E. D. Siggia, Phys. Rev. Lett. **62**, 1564 (1989).
[51] C. L. Kane *et al.*, Phys. Rev. B **41**, 2653 (1990).
[52] A. Auerbach and B. E. Larson, Phys. Rev. B **43**, 7800 (1991).
[53] E. Arrigoni and G. C. Strinati, Phys. Rev. B **44**, 7455 (1991).
[54] C. Zhou and H. J. Schulz, Phys. Rev. B **52**, R11 557 (1995).
[55] V. J. Emery, S. A. Kivelson, and H. Q. Lin, Phys. Rev. Lett. **64**, 475 (1990).
[56] M. Marder, N. Papanicolau, and G. C. Psaltakis, Phys. Rev. B **41**, 6920 (1990).
[57] B. Nachumi, G. M. Luke, Y. J. Uemura, and S. Uchida (unpublished).
[58] G. M. Luke *et al.*, Physica C **185-189**, 1175 (1991).
[59] J. I. Budnick *et al.*, Europhys. Lett. **5**, 651 (1988).
[60] Y. J. Uemura *et al.*, Physica C **153-155**, 769 (1988).
[61] J. M. Tranquada, S. M. Heald, and A. R. Moodenbaugh, Phys. Rev. B **36**, 8401 (1987).
[62] T. Kamiyama *et al.*, Physica C **172**, 120 (1990).
[63] V. J. Emery and S. A. Kivelson (private communication).
[64] R. Pynn, W. Press, S. M. Shapiro, and S. A. Werner, Phys. Rev. B **13**, 295 (1976).
[65] S.-W. Cheong (private communication).
[66] Y. Koyama, Y. Wakabayashi, K. Ito, and Y. Inoue, Phys. Rev. B **51**, 9045 (1995).
[67] H. Yamaguchi, T. Ito, K. Oka, and H. Oyanagi, J. Phys. Soc. Jpn. **64**, 3614 (1995).
[68] Y. Ando *et al.*, Phys. Rev. Lett. **75**, 4662 (1995).
[69] Y. Ando, G. S. Boebinger, N. Ishikawa, and S. Uchida (unpublished).
[70] K. Takenaka, K. Mizuhashi, H. Takagi, and S. Uchida, Phys. Rev. B **50**, 6534 (1994).
[71] Y. Koike *et al.*, Physica B **213&214**, 84 (1995).
[72] V. J. Emery and S. A. Kivelson, Physica C **235–240**, 189 (1994).
[73] V. J. Emery and S. A. Kivelson, Phys. Rev. Lett. **74**, 3253 (1995).
[74] J. Zaanen, M. L. Horbach, and W. van Saarloos, Phys. Rev. B **53**, 8671 (1996).
[75] H. Eskes, R. Grimberg, W. van Saarloos, and J. Zaanen (unpublished).
[76] M. Salkola, V. J. Emery, and S. A. Kivelson, Phys. Rev. Lett. **77**, 155 (1996).
[77] F. Borsa *et al.*, Phys. Rev. B **52**, 7334 (1995).
[78] A. H. C. Neto and D. Hone, Phys. Rev. Lett. **76**, 2165 (1996).